ISSN 2709-4529

JOURNAL OF DIGITAL FOOD, ENERGY & WATER SYSTEMS (JD-FEWS)

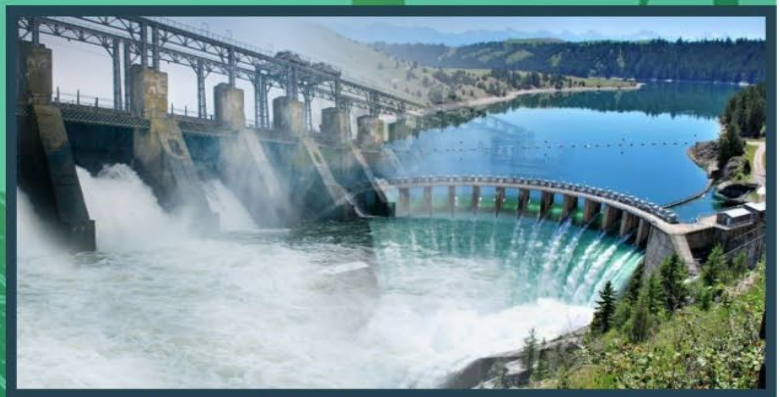

Vol.3 No. 1
June, 2022

About the Journal

The Journal of Digital Food, Energy & Water Systems (JD-FEWS) is a peer-reviewed bi-annual publication that publishes recent and innovative deployment of emerging digital technologies in Food, Energy, and WaterSystems. Food, energy, and water resources are interconnected scarce resources that require systems and technologies to foster sustainable management and effective utilization. The journal is also interested in articles that explore the nexus between at least two of these resources. Thejournal considers the following topics as long as they are deployed in the Food, Energy & Water space:

- Advanced Metering Infrastructure (AMI)
- Algorithm development
- Artificial Intelligence
- Blockchain and distributed ledger technology
- Case studies
- Cybersecurity
- Data mining & Big data
- Human-Computer Interaction
- Intelligent Forecasting
- Internet of Things
- Machine Learning
- Mathematical Optimization
- Robotics
- System architectures
- Wireless Sensor Networks

Editorial Team

Dr. Mohd Faisal Jalil

KIET Group of Institutions, India

Journal Manager

Mr. David, Love Opeyemi

University of Johannesburg, South Africa

Table of Contents

Volume 3 Number 1 JUNE 2022

ARTICLES

Journal of Digital Food, Energy & Water Systems, 3 (1): 1-15, 2022
ISSN 2709-4529

THE IMPACT OF CLIMATE CHANGE ON THE AVAILABILITY OF IRRIGATION WATER AT THE RIFT-VALLEY LAKES BASIN IN SOUTHERN ETHIOPIA: A REVIEW

Edmealem Ebstu TEMESGEN
Arba Minch University AWTI (Water Technology Institute), Arba Minch, Ethiopia
edmetemetsegiayu@gmail.com
Destaw Akili ARERU
Arba Minch University AWTI (Water Technology Institute), Arba Minch, Ethiopia
Demelash WENDEMENEH
Arba Minch University AWTI (Water Technology Institute), Arba Minch, Ethiopia

Abstract: Agriculture is one of the foremost climate-responsive businesses, with open-air production systems sensitive to temperature and rainfall. This paper reviews recent literature and assesses the impact of climate change on the accessibility of water resources for irrigation. The paper critically reviews recent research findings on climate change effect on the potential of surface water and groundwater for irrigation in Ethiopia's south rift valley (Abaya-Chamo) Sub-basin. Surface water in the south rift valley Ethiopia sub-basin, including the Abaya and Chamo lakes, is estimated to be just over 5,718 million m^3yr^{-1}. Finally, the implications for future study and development are emphasized. The effect of climate change (rainfall and temperature) on the water in the Abaya-Chamo lakes feeder Rivers is different for the near future (2021–2050) and extreme future (2071–2100) time using the RCP 8.5 scenario. Overall, findings show that the availability of water resources for irrigation purposes in the south rift valley Ethiopia sub-basin will be more vulnerable to changes in rainfall and temperature. In conclusion, Stream flow future projection (%) for each feeder river Bilate, Kulfo, Gidabo, and Hare are -9.07, -11.24, 3.89, 4.135, − 0.95, − 1.5, 13.4, and 15.4% respectively

Keywords: Abaya-Chamo, Climate change, Lake, River, Water Resource, irrigation

Journal of Digital Food, Energy & Water Systems, 3 (1): 1-15, 2022
ISSN 2709-4529

1.0 Introduction

Agriculture is one of the foremost climate-sensitive businesses, with open-air production systems that are amazingly delicate to temperature and rainfall. Climate change significantly affects crop yield by bringing down crop water use due to expanded evapotranspiration and changing precipitation patterns.

The influence of Climate change on water supplies is a hot point of investigation worldwide (Repel et al., 2007). Expanded warmth and decreased stream flow during the crop flowering season have a critical effect on crop yield. Expanding temperature may decrease the rural developing season and increment the number of water system days required.

Food uncertainty has resulted from climate inconstancy, especially precipitation changeability and going with dry seasons in Ethiopia (Rosell, 2011). As a result, irrigated farming is a critical technique for accomplishing food security by expanding rural generation, forcing cropping designs (number of crops per year), and utilising accessible irrigation water.

According to Tudorancea, and Taylor (2002), among twelve Ethiopian river basins Rift Valley basin is one of the basins with a chain of permanent lakes and tributary streams. According to the creator Wondwosen et al., (2015), the Ethiopian Rift Valley has interconnected lakes, tributary rivers, and groundwater. Abaya-chamo catchment is one of the rift valley basins called southern Rift Valley. It is found in southern Ethiopia.

The effect of climate change on stream flow and river accessibility for crop yield within the catchment of Abaya-chamo (Ethiopian Southern Rift Valley) was examined for its significance in expanding irrigation agricultural production yields within the area.

This paper aims to bring together information on the joins between climate change and the availability of water resources for irrigation within the southern Ethiopian Rift Valley basin based on academic literature.

2.0 Water on the surface of Abaya – Chamo sub-basin

According to Ayele et al., 2019 Southern Ethiopian Rift Valley catchment is a portion of the rift valley basin in Ethiopia, which is found within southern Ethiopia. Its' latitude ranges from 5°51.5'N to 8°8'N, and its longitude ranges from 37°16.3'E to 38°39.3'E, with an elevation run of 4200 m to 1108 m.

The yearly total precipitation ranges of the Ethiopian Southern Rift Valley sub-catchment is from 400mm-2300 mm. The Southern Ethiopian Rift Valley sub-basins water resources are divided into Chamo and Abaya lakes and their feeder streams. Southern Ethiopian Rift Valley lakes' total surface water resource is 5,718 million m^3yr^{-1}. This can be assessed utilizing the river's average flow into a system of lake

Journal of Digital Food, Energy & Water Systems, 3 (1): 1-15, 2022
ISSN 2709-4529

underneath "current" situations, counting agriculture and household water sources. (Mulugeta and colleagues, 2015; MoWE, 2012; Ermias Mekonnen, 2019).

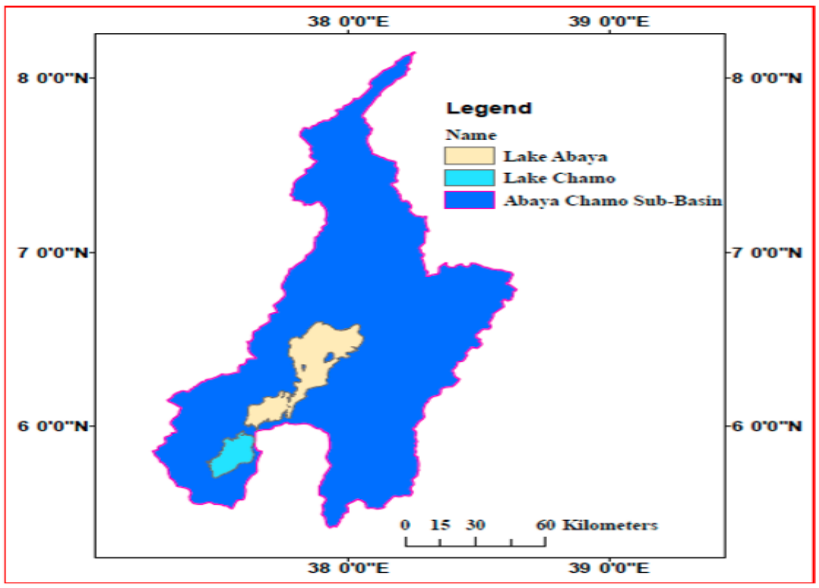

Figure 1. Southern Ethiopian Rift Valley Sub-Basin. (Source: (Ayele et al., 2019)

surface water of Southern Ethiopian Rift Valley sub-basin a tributary streams is additionally evaluated as the Min. stream flow discharge 3.5, 1.5, 2.9, 1.7, 1.8, and 0.85m^3s^{-1} and Max. Stream flow discharge 8.5, 3.9, 43.9, 9.1, 14, and 6.2 m^3s^{-1} Kulfo, Rabbit, Bilate, Gidabo, Gelena, and Kola separately (MoWR, 2008).

3.0 Climate Change on Southern Ethiopian Rift Valley Sub-basin water

Southern Ethiopian Rift Valley is generally composed of the two lakes and several rivers and streams that flow into them. Ethiopian precipitation within the Southern Ethiopian Rift Valley sub-basin described is lower average in most of the region, which is shown by direct to serious Dry spells periods. Dry spells happened nine times between 1988 and 2015, resulting in failure and serious food uncertainty. The precipitation data was measurably downscaled utilizing the NCEP-NCAR, and CanESM2 demonstrated predictions.

The extents of month-to-month measured and downscaled precipitation were exceptionally comparable. According to Beyene et al., (2021), the RCP2.6, RCP4.5, and RCP8.5 forthcoming scenarios were calculated to survey future dry spell designs. For a long time 2030; 2050; and 2080; the average yearly rainfall situation dropped by 0.2-13.7%; 0.5-6.4%; and 0.1-1.3% for the time of 2030; 2050; and 2080 individually.

Journal of Digital Food, Energy & Water Systems, 3 (1): 1-15, 2022
ISSN 2709-4529

3.1 Climate Swap on Chamo lake water availability

Chamo-lake is a portion of the most Ethiopian Southern Rift Valley category, which has 1108 m elevation.

Table1. Lake Chamo water by volume

Name	Area (km^2)	Maxi. Depth (m)	mean Depth (m)	Total Water Resource (Mm^3 per year)
Chamo	18,575	551	14.2 6	506

Source: Mulugeta et al., 2015; MoWE, 2012; and Ermias Mekonnen , 2019

According to Elias Gebeyehu (2017), the predicted stream flow within the 2030s and 2090s utilizing the RCM A1B scenario shows a decrease in runoff within the watersheds, specifically related to a diminish in rainfall and an increment in potential evapo-transpiration. Within the 2030s and 2090s, the mean yearly inflow is down 16.3% and 42.8%, individually, compared to the base period. In this scenario, evaporation over the lake is upgraded by 0.73 and 2.6 per cent within the 2030s and 2090s separately. Ungagged streams account for 32.1% of Lake Chamo's input, whereas gaged streams account for 67.9%.

Table 2. Lake Chamo water balance components and their value due to climate change ($mmyr^{-1}$).

component of water-balance	1996 to 2004	2030	2090
Areal rainfall of Lake	897.0	869.0	808.0
inflow River (Gauged)	161.0	153.0	98.0
river inflow (Ungauged)	96.0	62.0	49.0
evaporation from Lake	1217.0	1226.0	1249.0
outflow from Lake	Zero	zero	Zero

Source: Elias Gebeyehu , (2017)

3.2 Climate Variation influence on Lake Abaya water resource

Lake Abaya incorporates a surface estimate of $1160km^2$ and is found at an elevation of 1268 meters. Bilate Stream, which joins from the north and other streams from the south-east and South-west Mountains, nourishes the lake. The streams recharge to the Abaya Lake is 383,119,189 and 60 million cm for Bilate, Gelana, Gidabo and Hare, separately.

Journal of Digital Food, Energy & Water Systems, 3 (1): 1-15, 2022
ISSN 2709-4529

Table 3. Lake Abaya Water Resources

Name	Area (km^2)	Maxi. Depth (m)	Mean Depth (m)	Total Water Resource (Mm^3yr^{-1})
Abaya	1,162	24.5	7.1	2512

Source: Mulugeta et al., 2015; MoWE, 2012; and Ermias Mekonnen , 2019

4.0 Climate Change on Abaya-Chamo catchment Rivers water resource

4.1 Climate Change on Bilate River Water resource

According to Hailu et al. (2021), using RCP.4.5 and RCP.8.5 scenarios, climate change in 2021-2050 and 2051-2080 time was estimated by utilizing, and gathering means regional climate models as appeared in Table 4.

Table 4. climate change scenarios on (2021-2050) and (2051 -2080)

Scenario	Period							
PET (%)	ET (%)	SUR_Q (%)	GW_Q (%)		WYLD (%)	Rainfall (%)	Mean temp. (°C)	
RCP4.5	2021-2050	12	13.6	−7.15	8.22	−7.96	−27.11	0.7
	2051-2080	15	14	−10.25	−11.11	−9.22	−15.39	1.3
RCP8.5	2021-2050	14	14.7	−9.07	−10.46	−8.52	16.79	1.0
	2051-2080	19	13.9	−11.24	−12.54	−11.53	−46.26	2.0

According to Behailu et al. (2018) influence of climate changes on surface water was studied in Bilate catchment within the Ethiopian Southern Rift Valley watershed in Ethiopia. Using RCP.2.6 and RCP.8.5 model scenarios, the yield uncovers that annually stream decreases of up to 12.1 and 16.21% are possible. In any case, real abuse of these resources within the basin is very low, with domestic, animal, and minor agricultural operations accounting for 51.49 MCM (9.03%). Four scenarios were made in the basin up to 2035, each based on a particular set of assumptions. For the reference, in scenarios one, two, and three, total annual utilization is expected to be around 14.53, 20.43, 37.47, and 44.46%, respectively.

Table 5. Average yearly rainfall change of Bilate River up to 2035s

Hydrological parameter	Values' Simulated (mm)		Weighted average	% Rainfall
	Calibration	validation		
Evapotranspiration	772.50	769.60	7712.0	77.30

Total AQ recharge	123.70	116.50	120.20	12.0
Percolation	123.20	117.10	120.10	12.0
Shallow AQ recharges	105.20		102.90	10.30
Total water yield	93.80		101.40	10.10
Surface runoff	54.70	70.70	62.70	6.20
Base flow	40.0	40.0	40.0	4.0
Deep AQ recharges	6.20	5.50	6.0	0.60
Transmission losses	0.90	0.90	0.90	0.160
Groundwater evap.	1.50	0.70	0.710	0.070

AQ = Available discharge

According to Yoseph ArbaOrke and Ming-Hsu Li (2022), the Bilate Stream is the central water source for the encompassing populations' household and agriculture purposes. As a result, unpredictable precipitation and water shortage could critically affect agricultural productivity throughout crop developing seasons. Climate estimates in the future close 2021-2050 and distant future 2071-2100 duration were produced from Coordinated Regional Downscaling Try (CORDEX) Africa under two RCP,4.5, and RCP,8.5. With CORDEX-Africa data, the SWAT model was utilised to assess watershed hydrology changes.

To determine the characteristics of meteorological, hydrological, and agricultural dry spells, Standardized Precipitation Record (SPI), Stream flow Dry drought Record (SDI), and Observation Dry season File (RDI) were calculated. By the conclusion of the twenty-first century, evapotranspiration will have expanded up to 16.8% due to a huge rise in temperature. The yearly average precipitation is anticipated to decrease by 38.3% within the distant future time under RCP.8.5 model scenario, coming about in a 37.5% diminishment in stream flow. Diminished diurnal temperature run projections may advance crop development, but they may show expanded warm stress. The yearly mean stream flow within the Bilate watersheds declined by 3.64 $mmyr^{-1}$.

According to Getahun et al., a collaborative and combined of 20 Model Inter evaluation Forecast Stage5 (CMIP5), and common models circulation (GCMs) were utilized to produce 24 future climatic scenarios for the watershed in 2021, utilizing two figurative strength pathways and 6 GCM structure. The simulation of stream flow within the catchment and the soil and water assessment tool (SWAT) software were selected. Table 6. Show that the impact of climate varies on river flow in 2080.

Journal of Digital Food, Energy & Water Systems, 3 (1): 1-15, 2022
ISSN 2709-4529

Table 6. Climate change scenarios in the 2080s.

Parameter	Description	Process of model	range of Variation	Fitted value	Rank
CN2	SCS runoff curve number for moisture condition II	Runofl	-25 to +25		1
ESC0	Soil evaporator compensation factor	Evaporation	0 to 1	1*	2
Sd Awe	Availed soil water capacity	Soil water	-25 to +25	15a	3
Gwqmn	The threshold water level in the shallow aquifer for return flow to occur (mm)	Groundwater	0 to 1000	258*	4
Ch K2	Effective hydraulic conductivity in main channel alluvium (mm h ^{1})	Channel low	0 to 150	31a	5
Alpha Bf	Base how the recession is constant (days)	Groundwater	0 to 1	0.09	6
Ch N2	Manning's roughness coefficient for the main channel	Channel flow	0 to 1	0.43"	7
Surlag	Surface runoff lag coefficient	Runoff	0 to 12	9.64•	8
Gw Delay	Groundwater delay t me	Groundwater	0 to 10	6.45a	9
Rchrge Dp	Aquifer percolation coefficient	Ground-water	0-1	0.49a	

a=default values (absolute change); b= default values multiplied by one (relative change); c=defauk values are increased by this value (absolute change).

4.2 Climate Change on Kulfo River Water resource

According to Nega *et al*.,(2018), evaluating the potential effect of climate change action on river water resources is basic for future water resource plans and management. The future scenario for 2050 and 2080 river flow size within Kulfo watershed was explored utilizing a hypothetical climate vary scenario based on the Climate change of intergovernmental panel on (IPCC) fifth evaluation report predict the effect of climate variation on River flow.

The capacity affect of climate change on river flow was evaluated takes after: expanding temperature by 0.5°C from 2.5-3°C and 4.5-5°C, the average yearly flow on stream of the Kulfo River is anticipated within the 2050 to increase by 2.86% and 2080 by 2.99%; whereas from -10 to -20% by 10% drop rainwater come about in a stream diminishment by four per cent. The discharge of the Kulfo River has been observed to extend as precipitation increments and diminish when temperature increments within the twenty-first century. In general, the findings imply that the flow of streams within the Kulfo catchment will be more sensitive to precipitation changes than temperature changes.

4.3 Climate Change on Hare River Water resource

According to Biniyam Yisehak Menna (2017), downscaled climatic data (RCP.4.5 and RCP.8.5 scenarios) were utilized for the future period assessment. For RCP4.5 scenario, precipitation is anticipated to extend by 6.40, 2.56, and 16.30 per cent on a month-to-month premise within 2020, 2050, and 2080, respectively.

Journal of Digital Food, Energy & Water Systems, 3 (1): 1-15, 2022
ISSN 2709-4529

RCP8.5 scenario repeated the average yearly increment with 8.56, 8.08, and 15.85% within 2020, 2050, and 2080, respectively. The maxi. and min. Temperature projections for both RCP scenarios are predicted to rise with time. The month-to-month mean percentage changes in climate factors from the baseline period were utilized to model future stream flow estimates,. For RCP.4.5 scenario, the month-to-month mean stream flow is expected to extend by 12.2%, 8.0%, and 13.9%n from the standard period within 2020, 2050, and 2080, respectively, while for the RCP.8.5 scenario, it is projected to extend by 7.3, 13.4, and 15.4% within 2020, 2040, and 2080, respectively. Only future climate change conceivable outcomes were examined within the model runs, with all spatial data held constant.

Biniyam Y. and Abdella K. (2017) utilized bias-balanced RCPs climate data to assess the effects of climate variation on precipitation and flood rate within the Hare catchment. Future precipitation size changes in Peak flow amplitude and frequency are clearly governed Within the 2080s.

Table 7: Climate change effect on Rainfall and flood sizes at 2020, 2050 and 2080 periods.

period of Return		a. flood magnitude Change (%)					
		2	5	10	25	50	100
Period	2020	-3.58	-13 08	-20.94	-25.12	-29.63	-32.84
	2050	10.94	24	19.26	24.66	19.35	16.28
	2080	18.63	22.14	14.44	17.76	12.41	9.72

period of Return		b. Rainfall magnitude Change (%)					
		Two	Five	Ten	Twenty five	Fifty	One Hundred
Period	2020	-7.340	-16.750	-22.830	-30 010	-34.860	-39.340
	2050	9.960	13.90	14.20	12.970	11.450	9.480
	2080	27.150	25.840	22.450	16.810	12.210	7.460

4.4 Climate Change on Gidabo River Water resource

According to Beyene et al. (2021), the study determines the potential implications of climate swap on a hydro-climate pattern of variables at little sizes within the catchment of Gidabo. The MK drift of min. and max. temperature, as well as potential evapotranspiration (PET), appears that they are all growing, while precipitation (RF)

Journal of Digital Food, Energy & Water Systems, 3 (1): 1-15, 2022
ISSN 2709-4529

and stream flow are both diminishing irrelevantly additionally , the deviation to reference period of RF negative(58.7, 34.5, and 62.2percent); Temperature(T°) positive(1.15, 2.2and 4.2percent); PET positive(55.5, 73 and 99.9percent); and stream flow negative(2.63, 2.17 and 3.63percent) in Meso river; negative(0.27, 0.20 and 0.40percent) in Kolla river; positive (0.40, 0.13 and 0.53percent) in Apusto river; and negative (0.13, 0.10 and 0.03percent) in Bedessa river beneath RCP.2.6, RCP.4.5 and RCP.8.5 respectively. Hence, diminish in seasonal rainfall and the rise in To result in expanded potential evapotranspiration, which essentially impacts stream flow.

Table 8. climate change effect on future RF, PET, and temperature.

Period		Rainfall			Tmin.			Tmax			PET		
		2020	2050	2080	2020	2050	2080	2020	2050	2080	2020	2050	2080
RCP 2.6	Annual	-29.2	- 5.7	-82.1	1.1	0.9	1.3	0.9	0.9	] .4	40.6	62.6	48.5
	Spring	-0.7	4	-10.5	1	1.1	1.2	1	0.9	1.3	15.4	19.2	16.5
	Winter	-77.5	*40.8*	-97.7	1.1	0.9	1.4	1.2	1	1.6	17. 4	20.5	14.2
	Summer	11.9	-7.6	-44.7	1.1	1	1.4	1	1	1.5	7. 4	16.6	12
	Autumn	4b.2	38.6	30.8	1	0.9	1 .2	0.5	0.7	1.1	0.7	6.6	5.7
RCP 4.5	Annual	-91	- 64.7	-86.3	1.4	1.9	2.8	1.3	1.8	2.5	41.4	83.4	94.5
	Spring	0	7.1	-3.4	1. 3	1.9	2.9	1 .4	1 .8	2.6	11.4	21.1	23.4
	Winter	-82.7	-88.3	- 76.7	1 .4	2	2.8	1.5	2.1	2.9	13.7	26.7	30.6
	Summer	-30..8	-20.3	-4 3.7	1.5	1.9	2.7	1.5	2	2.8	10.5	21.4	24.1
	Autumn	22. 5	56.9	67.1	1.4	1.8	2.8	0.9	1.5	2	5.76	14.2	16.4
RCP 8.5	Annual	-56	- 33.1	-13.1	1.2	2.3	4. 1	1.1	2. 1	4.9	65.7	110	124.7
	Spring	-5.8	0.7	4.9	1. 4	2.3	4. 1	1.3	2	4.4	16.3	28.7	47.2
	Winter	35.3	-64.2	- 103. 3	1.2	2.3	4	1.1	2.4	4.3	21.3	37.9	57.2
	Summer	40.9	21.9	-53.8	1.2	2.2	3.9	1.2	2.2	4. 1	17.4	30.4	55
	Autumn	14.5	53.7	79	1.1	2.2	3.6	0.8	1.8	3.6	10.8	19	35.3

Amba Shalishe Shanka (2017) talks about the impressions of climate swap on runoff within the Gidabo River watershed. Daily rainfall and temperature within the river basin were downscaled utilizing the Statistical Downscaling Model version 5.1. To depict future climate change, HadCM.3 Ocean coupled atmosphere model output for

Journal of Digital Food, Energy & Water Systems, 3 (1): 1-15, 2022
ISSN 2709-4529

A.2a and B.2a scenarios determined. Climate swap scenarios for rainfall and To were developed for three future times: 2030, 2050, and 2080.

For both the A.2a and B.2a model scenarios, climate change action impact may result in increments in average monthly runoff within 2020, 2050, and 2080. The total average yearly runoff within the Gidabo stream basin is expected to extend by 3.4, 2.9, and 6.8percent within 2020, 2050, and 2080 respectively.

4.5 Climate Change on Gelana River Water resource

According to MoWR (2008), The Gelana Stream flows from the eastern to feed the Abaya Lak. The average yearly min., and max. Discharge is 0.5 and 12.5 $m^3s^{-1,}$ respectively.

5.0 Climate Change on Abaya –Chamo Sub-Basin Groundwater resource

According to Daniel et al. (2022), groundwater resource availability within the Southern Ethiopian Rift Valley Basin has been underweighted due to ongoing financial exercises and climatic change. Abaya–Chamo lakes basin's steady-state groundwater flow modelling. Moreover, the through-flow system in terms of groundwater flow direction and gradient, with groundwater flow from the high level toward the floor into the lakes from different directions with a high slope as shown in table 9.

Table 9. Water balance of Abaya Lake from ground water

Term of Flow	In	out	In- out
Storage	0.0E+00	0.0E+0	0.0E+0
Constant Head	1.970E+04	4.420E+06	- 4.40E+06
Horizontal Exchange	1.l50E+06	1.l70E+04	1.140E+06
Lower Exchange	3.270E+06	9.040E+03	3.260E+ 06
Recharge	3.770E+02	0.0E+00	3.770E+02
Saturation of the layer	4.440E+0	4.440E+00	1.0E+00
Discrepancy (%)	0		

Table10. Water balance of chamo Lake from ground water

Term of Flow	In	out	In-out
Storage	0.0E+0	0.0E + 0	0.0E+0
Constant Head	0.0E+0	5.710E + 05	- 5.710E+0
Horizontal Exchange	8.60E+04	4.750E + 0l	8.550E+04

Lower Exchange	4.850E+05	0.0E + 0	4.850E+05
Recharge	8.710E+01	0.0E + 00	8.710E+01
Sum of the layer	5.710E+05	5.710E + 05	0.0E+00
Discrepancy (%)	0		

6.0 CONCLUSION

There are several rivers and two lakes of various sizes in the Southern Ethiopian Rift Valley Basin. Though much of the blame may be attributed to rising demand, climate effect and variability will be found to place significant strain on Southern Ethiopian Rift Valley irrigation water.

Climate change has the potential to negatively affect water supply, stability, access, utilization, and demand in the Abaya chamo rift valley sub-basin. According to recent studies, the basin is extremely susceptible to variations in precipitation and temperature. As a result, river flows and runoff to lakes, as well as groundwater and lake water levels, are anticipated to fall in future and will be inadequate to meet the water demand of the country's population growth.

Climate change impacts agricultural land used for irrigation, making the design, operation, and management of water-use systems more difficult. As a result, livelihoods may be disrupted, poverty and marginalization of the poor may increase, and inequality may expand. Climate change is increasingly linked to many concerns and difficulties surrounding water resources. Climate risk is too costly to be tolerated, given the economic importance of water supplies, and immediate efforts to minimize the effects must be made using practical solutions.

The Abaya-chamo Sub-basin feeder Rivers have a maximum annual discharge of 3.5 m^3s^{-1} from the Kulfo River and a minimum annual discharge of 0.85 m^3s^{-1} from the Kola of flow water, as shown in table 11. The Bilate river has a maximum annual flow of 43.9 m^3s^{-1}, whereas the Hare river has a minimum annual flow of 3.9 m^3s^{-1}. Except for the Bilate and Kulfo rivers, most rivers have flow rates of less than $2m^3s^{-1}$ dry season period. During the dry season period, the flow rate of these rivers likewise diminishes. As a result, as indicated in table 8, this review seeks to the study influence of climate effect on river and lake water supply.

Table 11. Abaya-chamo Sub-basin Rivers discharge

Rivers	Kulfo	Hare	Bilate	Gidabo	Gelena	Kola
Min.discharge (m^3s^{-1})	3.5	1.5	2.9	1.7	1.8	0.85
Max.discharge (m^3s^{-1})	8.5	3.9	43.9	9.1	14	6.2

Journal of Digital Food, Energy & Water Systems, 3 (1): 1-15, 2022
ISSN 2709-4529

The considering of different base the climate effect on the annual water balance in Abaya-chamo lakes Feeder Rivers for future 2021–2050 and future 2071–2100 periods using RCP 8.5 scenario is tabulated below table 12.

Table 12. Climate change on the annual water balance

Rivers	years	Tmax future projection (%)	Tavg future projection (%)	Tmin future projection (%)	RF future projection (%)	PET Future projection (%)	Streamflow future projection (%)
Bilate	2050s	-	1	-	16.79	14	-9.07
	2080s	-	2	-	-46.26	19	-11.24
Kulfo	2050s	2.5	3.5	4.5	-10	-	3.89
	2080s	3	4	5	-20	-	4.135
Gidabo	2050s	2.1	-	2.3	-33.1	110	− 0.95
	2080s	4.9	-	4.1	-13.1	124.7	− 1.5
Hare	2050s	0.03^{o}c	-	0.15^{o}c	8.08	-	13.4
	2080s	0.11^{o}c	-	0.13^{o}c	15.85	-	15.4
Gelana	2050s	-	-	-	-	-	-
	2080s	-	-	-	-	-	-

7.0 RECOMMENDATIONS

In this study, climate change's effect on groundwater and the availability of some river bodies for irrigation like Gelana has been investigated. Future works can consider the effect of climate change on water resources for industrial & domestic purposes. Furthermore, the effect of climate change on lakes, feeder rivers and other water use projects in the future (2021–2050) and (2071–2100) needs to be studied.

REFERENCES

Abubakr Rahimi and Bayzedi. (2012). The Evaluation and Determining of Soil Inifiltration Models Coefficients. *Austalian Journal of Basic and Applied Sciences*, 94 - 98.

Amba Shalishe Shanka. (2017). Evaluation of Climate Change Impacts on Run-Off in the Gidabo River Basin: Southern Ethiopia . *Environment Pollution and Climate Change*, DOI: 10.4172/2573-458X.1000129.

Asma Dahak, Hamouda Boutaghane, and Tarek Merabtene. (2022). Parameter Estimation and Assessment of Infiltration Models. *Water* , 1185. https://doi.org/10.3390/w14081185.

Ayele Elias Gebeyehu, Zhao Chunju, Zhou Yihong & Negash Wagasho. (2019). Drought Event Analysis and Projection of Future Precipitation Scenario in Abaya Chamo Sub-Basin, Ethiopia . *J. Eng. Technol. Sci., Vol. 51, No. 5, 2019*, 707-728 .

Behailu Hussen, Ayalkebet Mekonnen, S. Pingale. (2018). Integrated water resources management under climate change scenarios in the sub-basin of Abaya-Chamo, Ethiopia. *Environmental Science*, DOI:10.1007/s40808-018-0438-9.

Beyene Akirso Alehu, Haile Belay Desta, and Bayisa Itana Daba. (2021). Assessment of climate change impact on hydro-climatic variables and its trends over Gidabo Watershed. *Modeling Earth Systems and Environment* , https://doi.org/10.1007/s40808-021-01327-w.

Biniyam Y. and Abdella K. (2017). The Impacts of Climate Change on Rainfall and Flood Frequency: The Case of Hare Watershed, Southern Rift Valley of Ethiopia. *Earth Science & Climatic Change*, DOI: 10.4172/2157-7617.1000383.

Biniyam Yisehak Menna. (2017). Simulation of Hydro Climatological Impacts Caused by Climate Change: The Case of Hare Watershed, Southern Rift Valley of Ethiopia. *Hydrology*, DOI: 10.4172/2157-7587.1000276.

Brouwer, C., K. Prins, M. Kay, and M. Heibloem. (1988). *Irrigation water management: Irrigation methods.* Rome: Food and Agric. Organ.

By J. Rockstrom, M. Falkenmark, C. Folke, M. Lannerstad, J. Barron, E. Enfors, L. Gordon, J. Heinke, H. Hoff, C. Pahl-Wostl. (2014). *Water Resilience for Human Prosperity. . .* New York: Cambridge University Press.

D. Daniel, T. Ayenew and Muralitharan Jothimani. (2022). Numerical ground water flow modelling under changing climate in Abay-chamo lakes basin, Rift Valley,Sourhern Ethiopia. *Environmental Science*, DOI:10.1007/s40808-021-01342-x.

Demelash Wondimagegnehu Goshime, Alemseged Tamiru Haile, Tom Rientjes, Rafik Absi, Beatrice Ledesert, Tobias Siegfried. (2021). Implications of water abstraction on the interconnected Central Rift Valley Lakes sub-basin of Ethiopia using WEAP . *Hydrology*, 2214-5818.

Edmealem et al. (2022). IMPACT OF DIFFERENT LAND USE CONDITION ON VERTISOLS INFILTRATION RATE AND MODEL PERFORMANCE IN DRY SEASON, SOUTHERN ETHIOPIA.

Elias Gebeyehu . (2017). Impact of climate change on Lake Chamo Water Balance, Ethiopia. *International Journal of Water Resources and Environmental Engineering*, 86-95.

Ermias Mekonnen . (2019). Surface Water and Groundwater Resources of Rift Valley Lakes Basin of Ethiopia: A Review of Potentials, Challenges and Future Development Perspectives. *Recent Development in Engineering and Technology*, 2347-6435.

FAO. (2009). *Food Security and Agricultural Mitigation in Developing countries.* Rome, Italy: www.fao.org/docrep/o12/i1318e00.pdf.

Getahun Garedew Wodaje, Z. Asfaw, M. Denboba. (2021). Impacts and uncertainties of climate change on stream flow of the Bilate River (Ethiopia), using a CMIP5 general circulation models ensemble. *Environmental Science*, DOI: 10.5897/IJWREE2020.0973.

Hailu Gisha Kuma, Fekadu Fufa Feyessa, and Tamene Adugna Demissie. (2021). Hydrologic resposes to climate change and land use/land cove changes in the Bilate catchment, Southern Ethiopia. *water and climate change*, doi: 10.2166/wcc.2021.281.

Horton RL. (1938). The interpretation and application of runoff plot experiments with reference to soil erosion problems. *340–349*.

Kostiakov AN. (1932). On the dynamics of the co-efficient of water percolation in soils. *In: Sixth commissio International Society of Soil Science*, Part A, pp 15–21.

M.L. Parry, O.F. Canziani, J.P. Palutikof, P.J. van der Linden and C.E. Hanson, eds,. (2007). *Assessment Report of the Intergovernmental Panel on Climate Change.* Cambridge, United Kingdom, and New York: Cambridge University Press.

MoWE. (2012). The Study on Groundwater Resources Assessment in the Rift Valley Lakes Basin in the Federal Democratic Republic of Ethiopia. Final REPORT . *JAPAN INTERNATIONAL COOPERATION AGENCY KOKUSAI KOGYO CO., LTD.* .

MoWR. (2008). Rift Valley Lakes Basin Integrated Resources Development Master Plan Study Project Phase 1 Final report. . *Halcrow, GIRD Consultants*.

Mulugeta Dadi Belete, Bernd Diekkrüger and Jackson Roehrig. (2015). Characterization of Water Level Variability of the Main Ethiopian Rift Valley Lakes. . *Hydrology*, www.mdpi.com/journal/hydrology.

Nega Gudeta Demmissie, Tamene Agugna Demissie,and Fayera Gudu Tufa. (2018). Predicting the Impact of Climate Change on Kulfo River Flow. *Hydrology* , 78-87.

Ogbe, V. B., Jayeoba, O.J. and Ode, S. O. (2011). Predictability of Philip and Kostiakov infiltration model under inceptisols in the Humid Forest Zone. *ISSN*(594 -602), 116-126.

Oku, E. and Aiyelari, A. (2011). Predictability of Philip and Kostiakov infiltration model under inceptisols in the Humid Forest Zone, Nigeria. *Natural Science, 45*(594 - 602), 594 -602.

Parveen Sihag, N.K. Tiwari and Subodh Ranjan. (2018). PERFORMANCE EVALUATION OF INFILTRATION MODELS. *J. Indian Water Resour. Soc.*, Vol. 38, No. 1.

Rashidi, M., Ahmadbeyki, A., and Hajiaghaei, A. (2014). Prediction of soil infiltration rate based on some physical properties of soil. . *Agricultural and Environmental Science*, 1359–1367 .

Rosell S. . (2011). Regional perspective on rainfall change and variability in the central highlands of Ethiopia . *Applied Geography* , 329-338.

Sunith John David, Akash Shaji,Ashmy M S. Neenu Raju, Nimisha Sebastian. (2018). A novel methodology for infiltration model studies. *International Journal of Engineering Technology and Managment Research*, 2454 - 1907.

Tudorancea, C. and Taylor, W. D. (eds.) . (2002). Ethiopian rift valley lakes. *Backhuys publishers, Leiden*, 259-271.

Wondwosen M. Syoum, Adam M. Mileweski and Micheal C. Durham. (2015). Understanding the relative impacts of natural processes and human activities on the hydrologythe Centeral Rift Valley lakes, East Africa. *Hydrol. Process.*, DOI: 10.1002/hyp.10490.

Yoseph ArbaOrke, and Ming-Hsu Li. (2022). Impact of Climate Change on Hydrometeorology and Droughts in the Bilate Watershed, Ethiopia. *Enviromental Science*, DOI: 10.3390/w14050729.

Journal of Digital Food, Energy & Water Systems, 3 (1): 16 - 28, 2022
ISSN 2709-4529

VERTISOLS INFILTRATION RATE AND MODEL PERFORMANCE EVALUATION OF VARIOUS LAND-USE CONDITIONS DURING SOUTHERN ETHIOPIA'S DRY SEASON

Edmealem Ebstu TEMESGEN
Arba Minch University Water Technology Institute, Arba Minch, Ethiopia
edmetemetsegiayu@gmail.com
Guchie Gulie SULLA
Arba Minch University Water Technology Institute, Arba Minch, Ethiopia
Guchie4@yahoo.com
Destaw Akili ARERU
Arba Minch University Water Technology Institute, Arba Minch, Ethiopia
Destaw2112@gmail.com

Abstract: The research was conducted on the field and models of vertisol soil types under varied land in southern Ethiopia's semi-arid Arba Minch university research centre site to measure infiltration and determine infiltration rates. The infiltration rate and model performance evaluation of the specific land use conditions affect the design and evaluation of surface and sub-surface irrigation methods. The infiltration rate is investigated on two different types of land (vegetable-covered land and bare land) and two different types of models (Horton and Kostiakov models). The experimental infiltration depth of the above soil conditions is measured using a double-ring infiltrometer. The research aims to figure out the field-measured infiltration rate, model infiltration rates, and basic infiltration rate, identify the impact of infiltration factors on infiltration rate, and find the best-fitted infiltration model. The findings from multiple infiltration models were compared with actual field data. The graphs of infiltration were generated to find the best fitting model for a certain vertisol soil type and two lands. The determination, correlation coefficient, bias, root mean square error (RMSE), model efficiency, determination coefficient (R^2), slope, correlation coefficient (r), average percentage error, and the gradient were the performance indicators examined for the optimum fitting of the model. The Kostiakov model's results are the best fit to observe field data for estimating infiltration rates at any given period in the research region by taking into account the infiltration numerical software performance indicators. The vegetable cover land infiltration rate is higher than un-disturbed bare land.

KEY WORDS: land use, Infiltration rate, model performance, Dry season, vertisols

Journal of Digital Food, Energy & Water Systems, 3 (1): 16 - 28, 2022
ISSN 2709-4529

1.0 INTRODUCTION

Water availability is critical for the development of agriculture and food security. The satisfaction of increasing population and per capita consumption demands forecasts that agricultural productivity will need to expand by 70% by 2050 (FAO, 2009). This population increase affects the hydrologic cycle from a local to a global scale through agricultural expansion (Rockstrom et al., 2014). The infiltration is the most significant process in the hydrologic cycle that affects agricultural water production (Brouwer et al., 1988). In recent years, the population has increased rapidly, and rising water consumers from many sectors have made the study region's water supply a cause of concern and conflict.

Surface irrigation system design and evaluation are simplified when infiltration modes simulate surface and subsurface flow. The soil's infiltration characteristics are quantified when in-situ infiltration data is computationally matched to models' infiltration (Oku E., and Aiyelari A., 2011). Several studies on different infiltration models have been conducted to determine model parameters, model effectiveness and applicability to various soil conditions and land uses (Abubakr Rahimi and Bayzedi, 2012; Asma et al., 2022; Ogbe et al., 2011; Sunith et al., 2018; Parveen et al., 2018; and Rashidi et al., 2014). They do not, however, consider the interplay between soil and agricultural land use factors in spatial variation. Additionally, despite these facts, no clear finding demonstrates infiltration capacity, the best fit model, and diverse land-use conditions of the study region's most prominent soil types (Vertisols).

As a result, developing models for specific time and space is critical for accurate in-situ quantification of this process. The study's objective was to determine the soils' infiltration capacity, model infiltration rate, evaluate infiltration factor on infiltration rate value variation, and choose the optimal infiltration model for the study location. Therefore, the infiltration rate of different land use and performance of infiltration models (Kostiakov, Horton's infiltration models) was investigated in this study using infiltration model performance indicators as tools under a vertisols soil type.

Journal of Digital Food, Energy & Water Systems, 3 (1): 16 - 28, 2022
ISSN 2709-4529

2.0 MATERIALS AND METHODS

2.1 Descriptions of the Study Area

The field experiment was implemented in the south-western zone of the South Nation and Nationality and People (SNNP) regional state at Arba Minch university demonstration farm, located 454 km south of Addis Ababa. Geographically, it is located at a latitude of 5°40'0" N to 6°20'0" N, a longitude of 37°20'0" E to 37°40'0" E, and an altitude of 1203m, as shown in Figure 1.

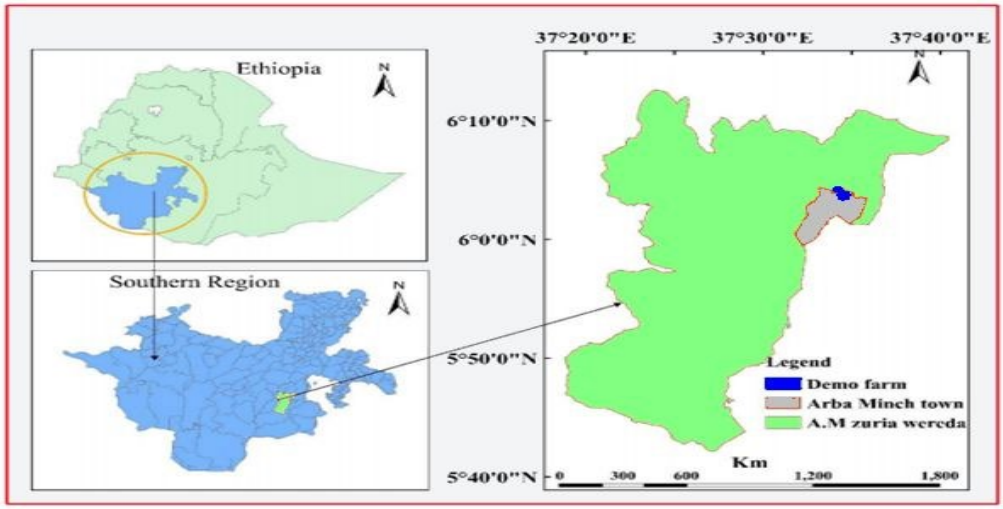

Figure 1. The study area Location map

2.2 Treatments' design and setting

The treatment of this study consists of one field infiltration measurement method (Double Ring infiltrometer method), two types of land use conditions (bare and vegetable cover land), and a vertisol soil type, which were used for the measurement of all infiltration data. There were a total of 4 samples for each land use condition site.

The double ring infiltrometer instrument was settled and driven 15cm deep into the soil. The size of the infiltrometer is 25cm in-depth, 30 cm in inner and 60 cm in outer diameter.

2.3 Materials to Conduct an Infiltration Test

- **The infiltrometer (double ring)** has a diameter of 30 & 60 cm and a 25cm height.
- **A hammer** is used to drive the ring into the soil.
- **A spade** is used to collect soil samples from the site to determine physical properties.
- **Bags** are used to transport soil samples to the laboratory.
- **A transparent ruler** measures the amount of water depleted in the soil with respect to time.

Journal of Digital Food, Energy & Water Systems, 3 (1): 16 - 28, 2022
ISSN 2709-4529

- **A Stop Watch** is used to read the proposed time.
- **A sufficient amount of water** is added to rings for depletion measurement
- **Plastic wrap** is used to prevent soil disturbance during the initial water application

2.4 Infiltration Models

The following infiltration models were evaluated to determine which model is the best fit for the experimental field infiltration rate:

Horton's model: Horton described the loss of infiltration capability as an exponential drop over time and generated the following equation (Horton RL., 1938)

$$f = fc + (fo - fc)e^{2-kt} \quad (1)$$

Where: f = infiltration capacity at any time t; fc = final steady-state infiltration capacity; fo = initial infiltration capacity; k = Horton's constant representing the rate of decrease in infiltration capacity; t = time in hours.

Kostiakov model (Kostiakov AN, 1932)

$$f = at^b \quad (2)$$

Where: f = cumulative infiltration at any time t; a and b = constants, t = time in minute,

Model Performance Indicators: Two infiltration models (Horton, and Kostiakov) were evaluated with the comparison of field observed infiltration rate simultaneously using the infiltration parameters. Several researchers used a variety of statistical methods for comparison of infiltration model performance like: Nash-Sutcliffe (NS), root means square error (RMSE), and determination coefficient (R^2) indicator (Parveen et al., 2018; Asma et al., 2022).

The R^2 and the RMSE were used to assess each model's goodness of fit in terms of how it describes the field measured infiltration well. The R^2 value reflects how well each model explains data variances, but the RMSE reveals how far the model results differ from the observed values. As a result, a high R^2 value near 1 and a low RMSE value around 0 both imply that the anticipated and observed infiltration curves are in good agreement.

The RMSE is a measure of the difference between projected and measured values and is widely used to assess the exact hydrology models. The RMSE formula describes as follow:

$$\boldsymbol{RMSE} = \sqrt{\frac{(\sum_{i=1}^{n}(pi-oi)^2)}{n}} \quad (3)$$

Where: Pi is Predicted results; Oi is Measured results, and n is the measurements number

Determination coefficient (R^2) is the predicted value of the infiltration rate plot versus observed values. Its value is greater than 0.75, indicating that the best fit to the observed data is described as the following formula.

$$R^2 = 1 - \frac{SSE}{SST} \quad (4)$$

Journal of Digital Food, Energy & Water Systems, 3 (1): 16 - 28, 2022
ISSN 2709-4529

Where: SSE is explained as the Sum of Square simulated data, and SST is the Total Sum of Square simulated data

The R^2 values indicate the degree to which each model explains data variations. RMSE shows the amount of divergence of the model values from the observed values.

Nash Sutcliffe: When comparing hydrological parameters, Nash-Sutcliffe is the most commonly utilized method. Nash-equation is:

$$NS = 1 - \frac{\sum_{ti=1}^{n}((yti^{m}) - yti)^2}{\sum_{ti=1}^{n}((yti - \bar{y})^2)} \quad (5)$$

Where: n is the observed data number; yti is the value of observation; yti^{m} is value of model, and y is the value of average observation

A very satisfactory performance indicates of Nash-Sutcliffe is above 90%, 80–90% value range indicates fairly good performance, and below 80% indicates an unsatisfactory fit.

Bias: it is the performance indicator of an infiltration model, which calculates the average difference between the observed and predicted index values. The bias value is zero, called "unbiased." It is defined by:

$$Bias = \frac{\sum_{i}^{n}(x-y)}{n} \quad (6)$$

Percentage average error is defined as follows:

$$PAE = \frac{\sum_{i=1}^{n}\left(\frac{x-y}{y}\right)}{n} * 100 \quad (7)$$

Where: PAE is average percentage error, x is values of observed data, y is values of computed data

Models selection criteria: the selection of the model's criteria are: they are most popular, simple, and applicable in the irrigation field, and the main one is to compare semi-empirical (Horton equation) and empirical (Kostiakov equation).

1.5 Data Collection and Analysis

Field infiltration tests, laboratory analysis, and documentation were all used to collect data. Soil infiltration rates were measured on two different soil types. The primary data for the infiltration test and the examination of soil physical parameters were obtained in the laboratory.

The soil infiltration rate of the study locations during the dry season was measured with a Double Ring Infiltrometer. For vegetable cover land conditions found at the Arba Minch demo farm, readings were obtained at regular intervals of 2, 5, 10, 20, 25, 30, 45, 60, and 80 minutes. Similarly, for bare land condition, which is found at Arba Minch demo farm,

Journal of Digital Food, Energy & Water Systems, 3 (1): 16 - 28, 2022
ISSN 2709-4529

infiltration data were taken at 2, 5, 10, 20, 25, 30, 45, 60, and 80 minutes until a steady infiltration rate is achieved on vertisol soil type.

3.0 RESULTS AND DISCUSSION

3.1 Field Measured Infiltration and Basic Infiltration Rate

The observed infiltration rate on vertisols for bare and vegetated land use conditions was calculated using the double ring method. It is shown in table 3.1, and the infiltration rate in vegetable-covered land is higher than in bare land throughout the same elapsed time interval.

Table 3.1 displays the experimental infiltration rate under different land-use.

Elapsed Time, min.	Elapsed Time, hr.	Cumulative Time, hr.	Cumulative infiltration (I) cm		Infiltration depth (d) cm		Infiltration rate (i) cm hr^{-}.	
			Vegetable cover land	Bare land	Vegetable cover land	Bare land	Vegetable cover land	Bare land
0	0	0	0	0	0	0	0	0
2	0.033	0.033	5.74	4.1	5.74	4.1	172.2	123
2	0.033	0.067	9.94	7.1	4.2	3	126	90
5	0.083	0.117	13.44	9.6	3.5	2.5	42	30
5	0.083	0.167	16.66	11.9	3.22	2.3	38.64	27.6
10	0.167	0.25	19.74	14.1	3.08	2.2	18.48	13.2
10	0.167	0.333	22.68	16.2	2.94	2.1	17.64	12.6
15	0.25	0.417	25.2	18	2.52	1.8	10.08	7.2
15	0.25	0.5	27.58	19.7	2.38	1.7	9.52	6.8
30	0.5	0.75	29.68	21.2	2.1	1.5	4.2	3
30	0.5	1	31.64	22.6	1.96	1.4	3.92	2.8
45	0.75	1.25	33.32	23.8	1.68	1.2	2.24	1.6
45	0.75	1.5	34.72	24.8	1.4	1	1.867	1.333
60	1	1.75	35.98	25.7	1.26	0.9	1.26	0.9
60	1	2	37.1	26.5	1.12	0.8	1.12	0.8
80	1.333	2.333	38.08	27.2	0.98	0.7	0.735	0.525
80	1.333	2.667	38.99	27.82	0.91	0.62	0.6825	0.465
80	1.333	2.667	39.89	28.43	0.9	0.61	0.68	0.4575

The final steady infiltration rate (i_c), and the initial infiltration rate (io), under different land-use conditions within vertisols, were calculated by a graphical approach. The vegetable-covered land basic infiltration rate and the initial infiltration rate values are 0.68 and 172.2 cm hr^{-} respectively, as well as the bare land basic (final) infiltration rate and initial infiltration

Journal of Digital Food, Energy & Water Systems, 3 (1): 16 - 28, 2022
ISSN 2709-4529

rate values, are 0.46 and 123 cm hr^{-1}, respectively. As the result, the value of the final and initial infiltration rates differ for all land use conditions.

The result observed that the initial and basic infiltration rates were higher in vegetable cove land than in bare land. There is a slight deviation for initial infiltration in the case of vegetable cove land and bare land, and the difference is (49cm hr^{-1}), but the basic infiltration rates difference is almost small (0.21 cm hr^{-1}) in both cases.

3.2 Modeling Soil Water Infiltration

The results of the computed values of infiltration rates using developed model equations for vegetable cover soil condition and bare land are tabulated in Table 3. 2. From the result, the values of infiltration rate of the Kostiakov model in both vegetable cover land and bare land are most closely matched to the field measured value compared to the Horton model throughout the same elapsed time interval.

Kostiakov model infiltration rates go to a constant at the time of 180 minutes for both vegetable land use conditions and undisturbed bare soil conditions, which is 0.798 cm hr^{-} and 0.56 cm $hr^{-1,}$ respectively. The Horton model basic constant infiltration rate for both vegetable soil use condition and undisturbed bare soil condition at the same time of 180 minutes is different at 0.74 cm hr^{-} and 0.52 cm hr^{-1}. respectively.

Therefore, the basic constant rate of infiltration is different from model to model and different soil use conditions at the same measurement time and elapsed time.

Table 3. 2: Different model infiltration rate values.

Time, hr	Obs. infil. rate (cm hr^{-1})		Horton's infil. rate (cm hr^{-1})		kostikove infil. rate (cm hr^{-1})	
	vegetable cover land	bare land	vegetable cover land	bare land	vegetable cover land	bare land
0	0	0	0	0	0	0
0.03	172.2	123	159.33	114.04	270.14	194.28
0.067	126	90	144.51	103.67	107.51	77.1
0.12	42	30	124.84	89.86	51.1	36.56
0.16	38.64	27.6	107.86	77.89	31.81	22.72
0.25	18.48	13.2	84.56	61.4	18.55	13.23
0.33	17.64	12.6	66.33	48.43	12.66	9.02
0.42	10.08	7.2	52.05	38.21	9.41	6.76
0.5	9.52	6.8	40.88	30.17	7.38	5.25
0.75	4.2	3	19.95	14.95	4.31	3.06
1	3.92	2.8	9.91	7.52	2.939	2.084

Journal of Digital Food, Energy & Water Systems, 3 (1): 16 - 28, 2022
ISSN 2709-4529

1.25	2.24	1.6	5.1	3.9	2.18	1.55
1.5	1.87	1.33	2.79	2.14	1.71	1.21
1.75	1.26	0.9	1.69	1.28	1.4	0.99
2	1.12	0.8	1.16	0.86	1.17	0.83
2.33	0.735	0.525	0.85	0.61	0.95	0.67
2.67	0.68	0.465	0.74	0.52	0.798	0.56
2.67	0.675	0.4575	0.74	0.52	0.798	0.56

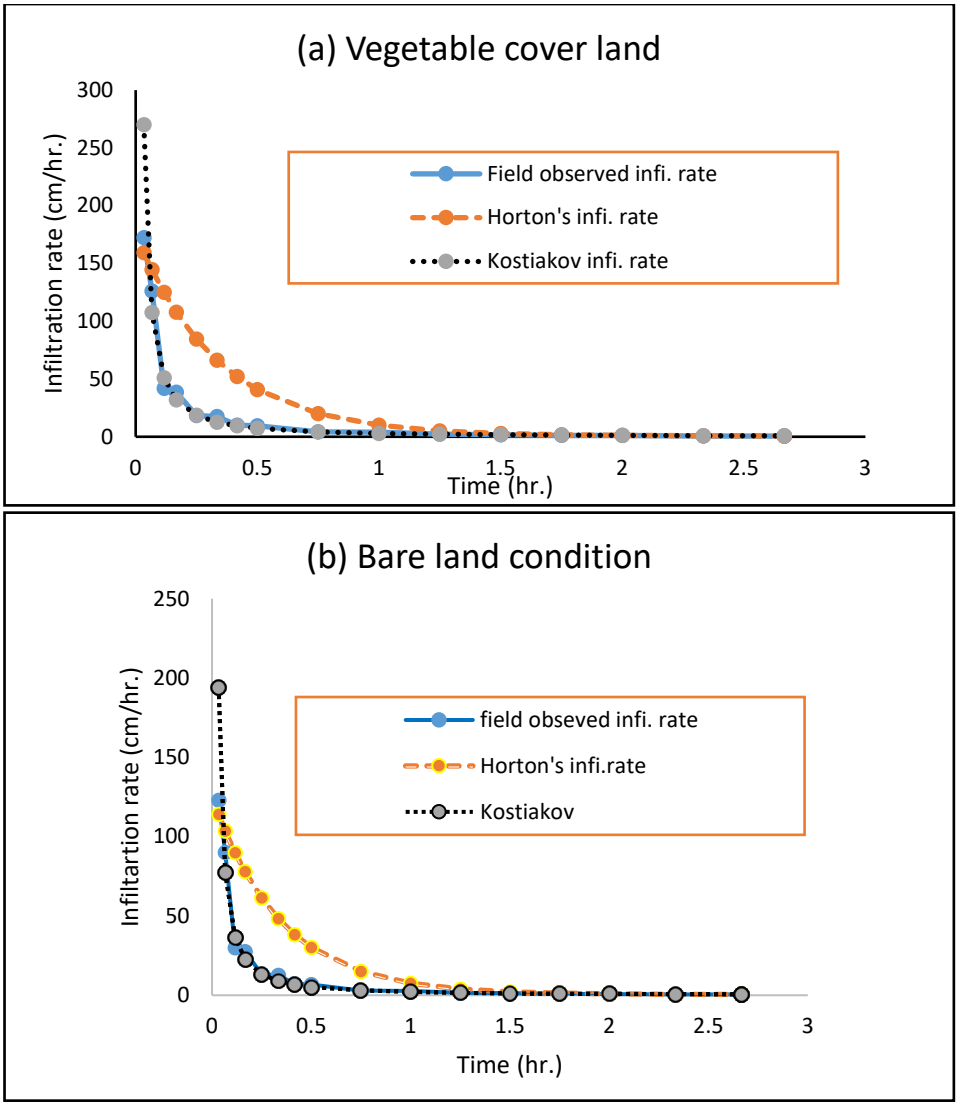

Figure 4. 1: Observed and model's Infiltration Rate: (a) Vegetable cover land and (b) Bare land

Journal of Digital Food, Energy & Water Systems, 3 (1): 16 - 28, 2022
ISSN 2709-4529

The values of the two infiltration model parameters, the basic infiltration rate i_c and the initial infiltration rate io under various land use conditions within vertisols, were determined by a graphical approach. From the results, the values of infiltration models are constant; the final and initial infiltration rates vary for all land use conditions and are presented in table 3. 3.

Table 3.3: Models' parameters, initial and final basic infiltration rates

Land use condition	Observed		Kostiakov				Horton's		
	i_o	i_c	i_o	i_c	a	b	i_o	i_c	k
Vegetable land	172.5	0.68	270.14	0.8	2.939	-1.33	159.33	0.74	-2.94
Bare land	123.5	0.46	194.28	0.56	2.084	-1.334	114.04	0.52	-2.87

Kostiakov and Horton's regional equations were generated from two land conditions (vegetable land cover and bare land) on vertisol soil type, shown in Table 3.4. The results of the generated equations were used to determine the Horton and Kostiakov model's infiltration rate in the study area.

Table 3. 1: Generated regional equation of Kostiakove and Horton equation.

Land use condition	Kostiakov	Horton's
	Generate equation	Generate Equation
Vegetable land	$i(t) = 2.939t^{-1.33}$	$i_t = 0.67+ 175e^{-2.94t}$
Bare land	$i(t) = 2.08t^{-1.334}$	$i_t = 0.46+ 125e^{-2.87t}$

3.3 Impact of Different Land Use on Infiltration Rate and Models

The impact of infiltration factors (vegetable cover and bare land condition) on the observed and model's infiltration varies with the same time interval, shown in table 3.5 and figure 4.2. The basic, initial, and instantaneous infiltration rates vary between the vegetable cover and bare land condition on observed, Horton's, and Kostiakov model results, which are presented in table 4 in per cent. The result shows that the factor of vegetable cover land condition contains high infiltration while bare land condition contains low infiltration, which varies between 67.65% and 70.2%; and 71.6 and 71.72% of the basic and initial infiltration rate, respectively.

Journal of Digital Food, Energy & Water Systems, 3 (1): 16 - 28, 2022
ISSN 2709-4529

Table 3.5: Infiltration variation vegetable cover and bare land condition on field observation, Horton's, and Kostialove models

infiltration condition	Field Observed		Kostiakov		Horton's	
	i_o	i_c	i_o	i_c	i_o	i_c
Vegetable cover land greater than Bare land infiltration rate (%)	71.6	67.65	71.72	70	71.57	70.2

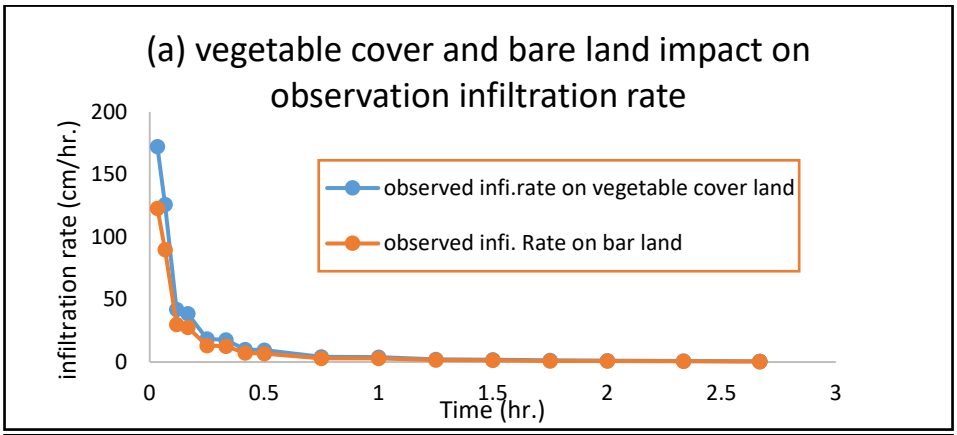

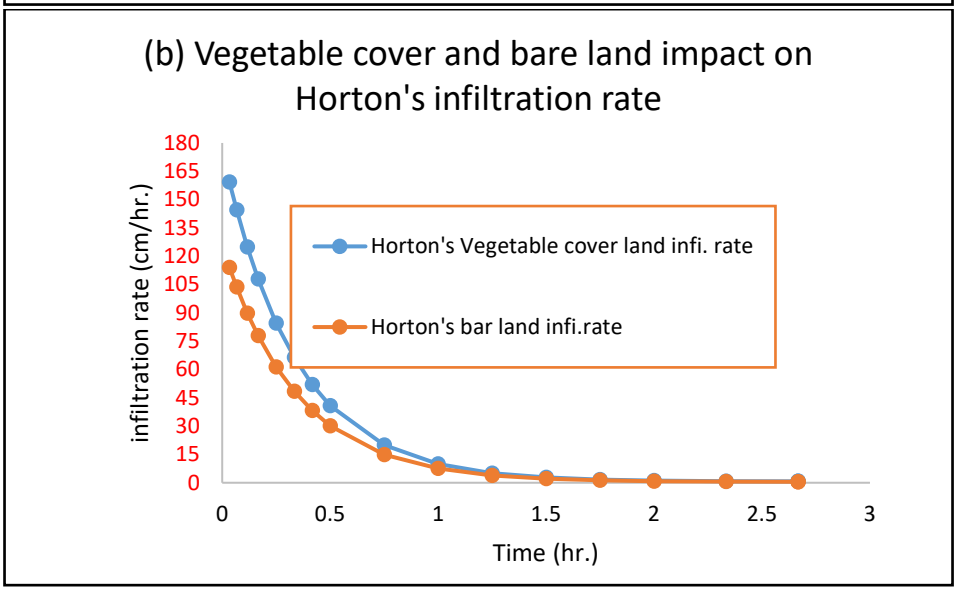

Journal of Digital Food, Energy & Water Systems, 3 (1): 16 - 28, 2022
ISSN 2709-4529

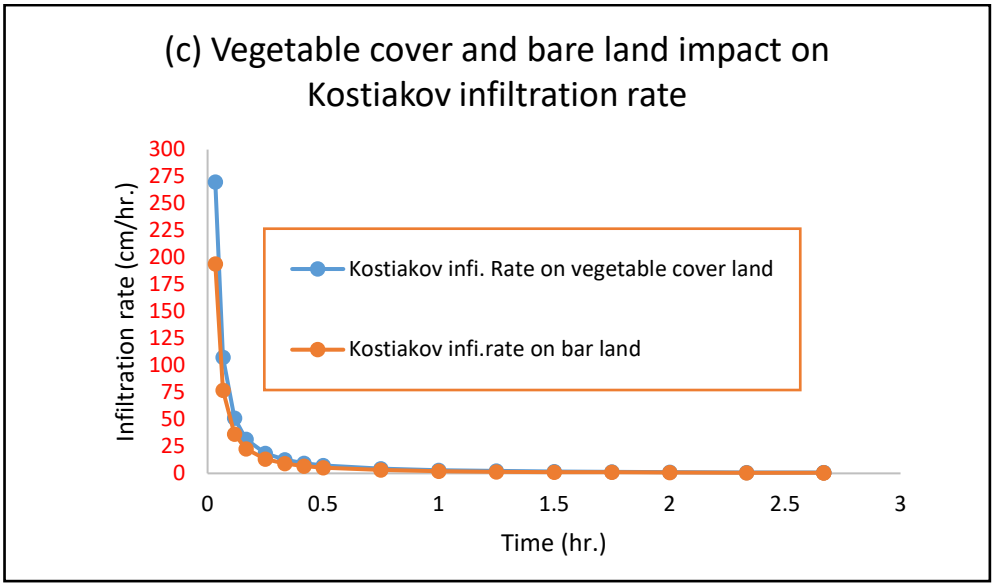

Figure 4. 2: vegetable cover and bare land condition impact on: (a) infiltration rate of observed, (b) infiltration rate of Horton's model, (c) infiltration rate of Kostiakov model

3.4 Model Performance Evaluation

The prediction was done using both empirical infiltration models (Horton's, and Kostialove) and compared with the field-measured cumulative infiltration. The infiltration models' performance was evaluated using bias, and root mean square error (RMSE), model efficiency, determination coefficient (R^2), slope, correlation coefficient (r), and average percentage error (PAE) statistical criteria. The best fit model was selected by considering infiltration model performance indicators like the minimum bias, average percentage error, root mean square error (RMSE), slope, and maximum model efficiency criteria, tabulated in Table 3.6.

The results are in table 3.6, which shows that for both land use (vegetable land and bare land) conditions, the Kostiakove model under: determination coefficient, correlation coefficient, bias, determination coefficient (R^2), root mean square error (RMSE), model efficiency, slope, correlation coefficient (r), average percentage error, and slope performance indicator consideration, is the best fit to the observed values, than Horton's model the study area.

Table 3. 2: The infiltration model performance indicators

Model performance indicator	Kostiakov		Horton	
	Vegetable cover land	Bare land	Vegetable cover land	Bare land
Coefficient of determination (R^2)	0.949	0.946	0.987	0.986
Slope	1.329	1.334	2.94	2.87

Correlation coefficient (r)	8.8E-06	1.7E-05	6.7E-06	1.3E-05
Roor mean squir error (RMSE)	35.92	26.2	24.37	17.71
Bias	-21.88	-16.1	-4.33	-3.18
Nash–Sutcliffe efficiency coefficient (NS)	41.81	42.3	73.22	73.63
Percentage average error (PAE)	-43.03	-44.7	2.06	2.07

4.0 CONCLUSION AND RECOMMENDATIONS

4.1 Conclusion

This study determined the infiltration rate on vegetable cover land and bare land using an infiltration factor, identified models' infiltration rates and evaluated the Horton's and Kostiakov infiltration models' performance on vertisols in Arbaminch southern Ethiopia. The double ring infiltrometer infiltration measure method was used on both vegetable cover land and bare land within the study area.

The results show that the constant or basic infiltration rates of the field observed, Korsakov and Horton's models on vegetable land-use conditions were 0.68, 0.8, and 0.74 cm hr^{-1}, and on bare, land conditions were 0.46, 0.56, and 0.52 cm hr^{-1}, respectively. It shows that different land conditions affect field infiltration rates as well as model infiltration rates. The vegetable land cover conditions considerably impacted the infiltration rate by increasing soil porosity, so vegetable cover soils showed more infiltration rate than bare soil conditions for both models and fields.

Infiltration models with field data use the determination coefficient (R^2), root means square error (RMSE), model efficiency, slope, correlation coefficient (r), percentage average error, and the slope performance indicator. After analysis, the values of the constant infiltration rate of vegetable cover land are higher than the bare land. The constant infiltration rates of both Horton and Kostiakov models vary from land use. It is observed that for both types of land use conditions, the infiltration rates for experimental data and models infiltration data do not exactly coincide. However, the kostiakov model, is more fit to observe field data than Horton's model in the study area.

4.2 Recommendations

The vegetable land cover condition had a considerable impact on increasing infiltration rate by controlling the runoff soil, so vegetable cover soils showed more infiltration rate than bare soil conditions in vertisols during dry seasons. So we utilized different infiltration rate for their design and evaluated surface irrigation methods on both vegetable land use conditions and bare land.

The best-fitting model in the study area is kostiakov Model for both vegetable land cover and bare land use conditions by considering Bias, root mean square error (RMSE), model efficiency, determination coefficient (R^2), Slope, Correlation coefficient (r), average percentage error, and the slope performance indicator. Therefore, compared to that Horton's

model, the kostiakov infiltration model is recommended to calculate the infiltration rate of Vertisols for the dry season.

We recommend that further study can identify other hydrologic processes, addressing additional land use conditions, soil type, model performance indicator, infiltration measurement methods, and all infiltration factors during both dry and wet seasons.

REFERENCES

Abubakr Rahimi and Bayzedi. (2012). The Evaluation and Determining of Soil Inifiltration Models Coefficients. *Austalian Journal of Basic and Applied Sciences*, 94 - 98.

Asma Dahak, Hamouda Boutaghane, and Tarek Merabtene. (2022). Parameter Estimation and Assessment of Infiltration Models. *Water* , 1185. https://doi.org/10.3390/w14081185.

Brouwer, C., K. Prins, M. Kay, and M. Heibloem. (1988). *Irrigation water management: Irrigation methods.* Rome: Food and Agric. Organ.

By J. Rockstrom, M. Falkenmark, C. Folke, M. Lannerstad, J. Barron, E. Enfors, L. Gordon, J. Heinke, H. Hoff, C. Pahl-Wostl. (2014). *Water Resilience for Human Prosperity. . .* New York: Cambridge University Press.

FAO. (2009). *Food Security and Agricultural Mitigation in Developing countries.* Rome, Italy: www.fao.org/docrep/o12/i1318e00.pdf.

Horton RL. (1938). The interpretation and application of runoff plot experiments with reference to soil erosion problems. *340–349*.

Kostiakov AN. (1932). On the dynamics of the co-efficient of water percolation in soils. *In: Sixth commissio International Society of Soil Science*, Part A, pp 15–21.

Ogbe, V. B., Jayeoba, O.J. and Ode, S. O. (2011). Predictability of Philip and Kostiakov infiltration model under inceptisols in the Humid Forest Zone. *ISSN*(594 -602), 116-126.

Oku, E. and Aiyelari, A. (2011). Predictability of Philip and Kostiakov infiltration model under inceptisols in the Humid Forest Zone, Nigeria. *Natural Science, 45*(594 - 602), 594 -602.

Parveen Sihag, N.K. Tiwari and Subodh Ranjan. (2018). PERFORMANCE EVALUATION OF INFILTRATION MODELS. *J. Indian Water Resour. Soc.*, Vol. 38, No. 1.

Rashidi, M., Ahmadbeyki, A., and Hajiaghaei, A. (2014). Prediction of soil infiltration rate based on some physical properties of soil. . *Agricultural and Environmental Science*, 1359–1367 .

Sunith John David, Akash Shaji,Ashmy M S. Neenu Raju, Nimisha Sebastian. (2018). A novel methodology for infiltration model studies. *International Journal of Engineering Technology and Managment Research*, 2454 - 1907.